Light manipulation using organic semiconducting materials for enhanced photosynthesis

Jackie Zorz (jacqueline.zorz@ucalgary.ca)
University of Calgary https://orcid.org/0000-0001-6892-0936
William Richardson
University of Calgary
Audrey Laventure
Université de Montréal https://orcid.org/0000-0002-0867-0231
Marianne Haines
University of Calgary
Edward Cieplechowicz
University of Calgary https://orcid.org/0000-0001-5466-9103
Alireza Aslani
University of Tehran
Agasteswar Vadlamani
University of Calgary
Joule Bergerson
University of Calgary https://orcid.org/0000-0002-4736-3509
Greg Welch
University of Calgary
Marc Strous
University of Calgary https://orcid.org/0000-0001-9600-3828

Article

Keywords: light manipulation, organic semiconducting materials, photosynthesis, photosynthetic microorganisms

Posted Date: October 28th, 2020

DOI: https://doi.org/10.21203/rs.3.rs-90447/v1

Version of Record: A version of this preprint was published at Cell Reports Physical Science on April 1st, 2021. See the published version at https://doi.org/10.1016/j.xcrp.2021.100390.

Light manipulation using organic semiconducting materials for enhanced photosynthesis

Jackie Zorz[1], William D.L. Richardson[1], Audrey Laventure[2,3], Marianne Haines[1], Edward Cieplechowicz[2], Alireza Aslani[4,5], Agasteswar Vadlamani[1], Joule Bergerson[4], Gregory C. Welch[2], Marc Strous[1]

[1]Department of Geoscience, University of Calgary, Calgary, AB, T2N 1N4, Canada

[2]Department of Chemistry, University of Calgary, Calgary, AB, T2N 1N4, Canada

[3]Département de chimie, Université de Montréal, succursale Centre-ville, Montréal, QC, H3C 3J7, Canada

[4]Departement of Chemical and Petroleum Engineering, University of Calgary, Calgary, AB, T2N 1N4, Canada

[5]Department of Renewable Energies and Environment, University of Tehran, Tehran, Iran

Abstract

Photosynthetic microorganisms, such as algae, are sources of bioproducts and pharmaceuticals. As they require only sunlight and carbon dioxide to grow, they have potential for future mitigation of CO_2 emissions. However, inefficiencies in the growth of these organisms remains an issue for realizing these emission reductions, primarily in terms of photosynthetic efficiency, photoinhibition, and photolimitation. Here, we show how the use of light filtration through semi-transparent films comprised of organic π-conjugated molecules and subsequent organic photovoltaic devices, has the potential to improve the photosynthetic efficiency of algae, and the total power generation of a combined organic photovoltaic/algae system. Experimental data is used to fit a photosynthetic model predicting algal photosynthetic growth given light intensity and light transmission through an organic photovoltaic device. This work demonstrates the feasibility of using a system combining photosynthetic growth with electricity-producing organic photovoltaics and provides a template for exploring other blended applications of these technologies.

Main

The mass cultivation of photosynthetic microorganisms, collectively referred to herein as "algae" is of interest to agricultural, pharmaceutical, and energy industries. However, challenges including suboptimal photosynthetic efficiency and high operating expenses persist in large scale operations[1,2]. This results in a high price point for algae feedstock, which makes algae biomass currently unsuitable for biofuel applications[3,4].

The theoretical maximum efficiency of photosynthesis has been estimated between 8-12%, but in practice, photosynthetic efficiency is often much lower, around 1%[5,6,7]. In algae, high photosynthetic efficiency is only realized at very low light intensities[8], but can be improved by using red light, at wavelengths close to those absorbed by reaction-center chlorophyll and accessory light-absorbing pigment molecules[7,9,10,11,12]. For photosynthetic applications of algae, the obvious choice for an abundant and sustainable light source is sunlight. However, direct sunlight encompasses the entire spectrum and has high intensity, causing photoinhibition and decreases in photosynthetic efficiency, in some cases completely killing algae cultures[13].

Similar to photosynthesis, photoexcitation of the materials in organic photovoltaic devices (OPVs) induces charge separation, which can subsequently be used for conversion of light energy into usable electricity. OPVs have active layers comprised of organic π-conjugated materials (typically polymers or small molecules) that can be tailored to absorb light at desired wavelengths, while remaining transparent in other parts of the spectrum[14,15,16].

Here we investigate if OPVs, when used as electricity-producing light filters, improve the feasibility of algae biotechnology. We explore through experiments and modeling, if this combination of technologies increases solar power conversions, leading to the potential for energetic gains by co-producing electricity. For photosynthesis, we use a microbial consortium obtained from alkaline soda lakes[17], mainly consisting of *Phormidium* cyanobacteria (a blue-green algae). This cyanobacterial

consortium has been shown to be ecologically robust[12] and facilitates direct air capture of CO_2[18]. The cyanobacterium reaches its maximum photosynthetic rate at a light intensity that is about 10% that of direct sunlight[18], thus making it an ideal candidate to test if light filtering improves growth.

Light filters are photoprotective at high light intensities

To investigate the potential benefits of combining growth of the cyanobacterial consortium ("algae" for simplicity) with a light filter, we performed a series of outdoor algal cultivations and used the measured results to generate a photosynthetic model. The light filter used with the cultivations was prepared with the organic π-conjugated perylene diimide dimer derivative, $tPDI_2N$-EH, herein simply referred to as PDI, as the active chromophore[19,20] (Figure 1, Supplementary Figure 1). Perylene diimides are a suitable chromophore for light absorption between 450 and 550 nm, have excellent thermal and light stability properties, and as such have been widely used as an active material in photovoltaic cells[21,22,23]. We use this light filter as a proof-of-concept platform that has the potential for transitioning into an OPV module, where it could be endowed with the dual-function of filtering out the wavelengths of light that are unnecessary or detrimental to algae growth while converting the absorbed light energy into electricity. This selected PDI material can be made on scale, is an effective non-fullerene acceptor in air processed and stable OPVs, and is compatible with roll-to-roll coating on flexible and lightweight transparent substrates, such as polyethylene terephthalate (PET)[24,25,26] . The light filter construction methods parallel those used to fabricate OPV modules (Figure 1, Supplementary Figure 2). The intensity of the light filter transmission was modulated by varying the concentration of the PDI coating solutions. In total, three light filters, referred to as LF-1, LF-2 and LF-3, were prepared using three densities of coating solution concentration (corresponding to 70, 50 and 30% light transmission respectively) (Figure 1).

Algal cultures were grown both in direct sunlight and within a greenhouse structure in separate trials, and in each trial, the three densities of light filter were tested along with a filter-free control (Figure

1, Supplementary Figure 3). To relate the results of these experiments to other photosynthetic species, the electron transport kinetics of the algae were measured (Supplementary Figure 4). The relationship between electron transport kinetics and light intensity of the algae behaved as expected: an initial positive relationship between light intensity and photosynthetic activity, followed by a plateau once maximum rates of photosynthesis were achieved, followed by a decrease in photosynthetic activity (photoinhibition) as light intensity became damaging[13,27].

Outdoor experiments demonstrated that the light filters promoted photosynthesis when initial biomass concentration was low (< 0.1 g/L dry weight), and when incident light intensity was high (Figure 2). At these high light intensities, daily photosynthetic production was between 1.3-4.7X greater with light filters than without (Figure 2). During the trial at the highest incident light intensity, the light filters prevented complete photobleaching and death of the algae cultures (Supplementary Figure 5). The discrete chromophore density of the light filter did not directly affect photosynthesis (Figure 2), but rather photosynthesis was affected by the amount of light reaching the bioreactor. The effect of light on photosynthetic production was explored further by developing a model based on these experimental results.

Modeling photosynthetic growth with experimental measurements

To define the conditions in which light filters would be advantageous for growth, a Type II bulk photosynthetic productivity model was created and fit to the experimental data[28]. This model determines the photosynthetic output of the cyanobacterial consortium given light intensity, biomass density, filter transmission, and bioreactor depth. Algae are generally grown in open raceway ponds or closed bioreactors, depending on the application, and light filters could be integrated with either approach. Here we model the growth of algae in ponds, accounting for the fact that as light travels through the pond, it gets absorbed and attenuates (Supplementary Figure 6).

Integration of model predictions over a hypothetical pond of 20 cm depth showed that maximum photosynthetic output is largely influenced by initial biomass concentration (Figure 3bc). Biomass concentrations of 0.1 g/L and 0.5 g/L were chosen, roughly corresponding to the biomass concentration expected during inoculation and harvest, respectively[29]. The model showed that light attenuation within a 20 cm pond is more limiting to photosynthetic output than photoinhibition, at both inoculum and harvest biomass concentrations. Therefore, filtering of incident light generally reduced photosynthetic productivity. However, even with a pond depth of 20 cm, at lower biomass concentrations (Figure 3b), the use of filters (> 50% transparency) had little effect on maximum growth in high light intensity (> 500 W/ m^2). Even with very high biomass concentrations (Figure 3c) there remains a level of filter transmission (> 75%) that would also have no effect on photosynthetic growth at very high light intensities (> 700 W/m^2). To positively influence photosynthetic efficiency using a light filter with 60% transmission in full sunlight of 1000 W/m^2, a pond shallower than 9 cm (0.3 g/L culture density), or a culture density less than 0.13 g/L dry weight (20 cm deep pond) would be required.

Increased power production with combined OPV and photosynthesis

A comparative analysis was conducted to determine if combining the light filter (as part of an OPV device) with photosynthetic growth would be a worthy exercise strictly in terms of the amount of power generated. A model OPV device with 40% transmission was prepared using the PDI derivative, acting as a non-fullerene acceptor, in combination with high performance and commercially available PTQ10 polymer, acting as an electron donor[30,31,32,33,34] (Supplementary Figure 2). For our proof-of-concept devices, PTQ10 was selected as a donor polymer owing to a similar band gap and transmittance in the red region of the solar spectrum to PDI[33]. In addition, OPVs based on this polymer exhibit high operating voltages and can be made on scale via roll-to-roll compatible methods. An estimate for power conversion efficiency of 4.2% was obtained from calculations performed on the model OPV device

(Supplementary Table 1). We assumed the algae were grown in an open pond of 20 cm depth, with a dry weight biomass concentration increasing from 0.1 g/L to 0.5 g/L, as explained above. Four locations spanning 30 degrees of latitude in North America were chosen, and their average monthly solar radiation and day length were used to estimate photosynthetic output using the model (Figure 4a). The locations were Calgary Alberta Canada (51° N), Chicago Illinois USA (42° N), Phoenix Arizona USA (33° N), and Honolulu Hawaii USA (21°N). We also assumed an intrinsic caloric value for the biomass, based on the high heating value (HHV) of its organic material as a rough translation for its power potential[35,36]. In short, we estimated the average amount of electricity that could be produced by the model OPV with the absorbed light, and we estimated the amount of electricity that could be generated by combustion of the biomass grown with the remaining transmitted light.

The power analysis showed that the addition of an OPV device always resulted in higher combined OPV and algae power production than with photosynthesis alone (Figure 4bc, Supplementary Figure 7) and increased the overall efficiency of the system from less than 2% with algae alone to around 5% with algae and OPV (Figure 5c). The inclusion of the OPV device resulted in an increase in photosynthetic efficiency to above 2% (Figure 5a), but a decrease in biomass production that was 43-80% of its predicted maximum levels without light filtration (Figure 5b). Despite these losses in biomass production, any detriment to photosynthetic growth due to light filtering was more than compensated for by the power generation from the OPV device (Figure 4bc). Quantitatively, power production was predicted to increase by a factor of 2.2-4.8X when OPVs were added, and this effect was particularly prominent in the summer months when light intensity was highest (Figure 4b). Predicted power production of both OPVs and photosynthetic growth followed solar radiation trends and was highest in Phoenix, then Honolulu, Chicago, and Calgary (Supplementary Figure 7).

Discussion

The integration of light filters, particularly in the form of OPVs, into algal bioreactors has been proposed as a potential solution to improve photosynthetic efficiency and limit photoinhibition[37]. The combination of OPVs with algal bioreactors has the added benefit of concurrent electricity production on the same land area used for algae growth. Here, using both experiments and models, we investigated the effect of light filtration with an organic semiconducting light filter on the growth of a cyanobacterial consortium.

Light filters helped reduce the effects of photoinhibition in the outdoor experiments, mainly when light intensity was high and biomass concentration was low. Under these conditions, light attenuation due to self-shading from the algal cells was minimal, and growth was affected primarily by incident light intensity. Using the experimental results, a Type II photosynthetic model[28] was developed allowing for estimates of photosynthetic growth under realistic light and bioreactor conditions. An increase in photosynthetic efficiency was expected when the cyanobacterial consortium was grown with OPV light filtration compared to growth without (Figure 5a). The higher photosynthetic efficiency is due to the lower light intensity experienced by the algae after OPV light filtering[13]. Despite this increase in photosynthetic efficiency, total algal growth was expected to decrease under the conditions tested. In other words, with filtered light, the algae are able to grow proportionately more with the light received (increase in efficiency), but the amount of filtered light received is not enough to overcome photolimitation due to light attenuation with depth (decrease in growth). Regardless of losses in algal growth, combined power production from the model OPV device and biomass combustion was higher than for either technology on its own.

Higher power production for combined algae and OPV systems may already make the blend of these technologies advantageous for energy and agricultural industries. By applying the model developed here, it is evident that amendments to the pond and OPV light filter setup, like the use of a shallower bioreactor configuration (i.e. tubular or flat panel bioreactors), should be considered to improve photosynthetic growth with OPV light filters. There is also the possibility to apply OPV light filters periodically, only when culture density is low after inoculation or on very sunny days. Alternatively, different organic

compounds could be chosen for the construction of the OPV active layer. Organic molecules have been developed recently that target wavelengths in the infrared region (> 700 nm), thus absorbing light outside the range of photosynthetically active radiation (400-700 nm)[38,39,40,41,42]. Targeted enhancement of metabolite production presents another avenue to pursue for the incorporation of light-filtering OPV devices, as the use of coloured light has been shown to increase production of certain high valued products, such as pigments or fatty acids[7,37,43]. Therefore, the optimal solution for incorporating OPV devices with photosynthetic growth will be case specific and depend on many factors including the intended product.

Presently, commercially available inorganic photovoltaic modules are achieving efficiency values of 10-20%, several times higher than the predicted efficiency for the combined OPV/algae system here (~5%). However, semi-transparent OPV modules and photosynthetic systems offer benefits over opaque inorganic photovoltaics, such as mass production using additive manufacturing methods which have a low energy input and use low capital equipment allowing for localized production[44,45]. OPVs are also primarily comprised of earth abundant and non-toxic materials leading to low cost/safe devices which can be easily disposed of or recycled[46]. OPVs can be tailored to the specific needs of the system, and thus are of interest in alternative applications where some degree of transparency or a certain aesthetic is required (e.g. window coverings and greenhouses)[47,48,49,50,51]. Additionally, the photosynthetic portion of such a combined system could be filled by a number of algal and agricultural candidates, from algae grown to produce biofuels and bioproducts, to crops grown for a variety of agricultural and commercial functions, further expanding potential applications for these technologies[52]. Growth of algae is of particular interest due to their high biomass yields, potential for growth using reclaimed water and nonarable land, applications in wastewater remediation, as well as their vast genetic potential for producing various bioproducts[3].

Recently, research has targeted the combination of organic semi-transparent filters with greenhouses, growing plants[47,51,52,53], and single algal strains[10,54], suggesting that there is interest in combining solar power with the growth of photosynthetic organisms. In agreement with our findings, Michael *et al.*

(2015)[54] showed decreased algal growth with light filters when algae were grown in flasks, but an increase in growth in flat panel bioreactors, presumably due to the small path length of the flat panel bioreactor. Similarly, Detweiler *et al.* (2015)[10] used dilute, small volume algae cultures and found equal performance of cultures grown with and without light filters. The idea to combine OPV technology with photosynthetic organisms is relatively new, and most of this research relies strictly on theoretical modeling or lab-scale experimental data, without providing an intersection of these two approaches. The present study demonstrates that light filters can promote photosynthesis experimentally, and also provides a framework for developing system specific models to analyze and design future combinations of photosynthetic growth and OPV technologies.

Methods

Algae cultivation

Cultures of a cyanobacteria (a blue-green algae) dominated consortium previously enriched from Canadian soda lakes[12,17] were grown with constant stirring in glass, airtight vessels. The cyanobacterial species grown here is filamentous and from the genus *Phormidium.* The high pH media used for growth contained 5.88 mM $NaNO_3$, 0.92 mM NH_4Cl, 1.00 mM $MgSO_4$-$7H_2O$, 0.17 mM CaCl-$2H_2O$, 0.43 mM NaCl, 1.44 mM KPO_4 dibasic, 6.04 mM KCl, 179.28 mM Na_2CO_3, 142.85 mM $NaHCO_3$, 0.01 g/L ferric ammonium citrate, and 1mL/L of trace element solution. Initial pH of the media was 10 ± 0.1. When used, the light filters were placed directly on top of the bottles to ensure that all incoming light was filtered (Supplementary Figure 3*)*. Between experiments, initial biomass concentrations, bottle shape, daylight hours, and light source varied as shown in Table 1. All experiments were conducted in Calgary, Alberta, Canada during the months of May-September.

To begin experiments, a known weight of biomass from a stock culture was added to a mixing bottle containing a known volume of media. This bulk solution was then evenly distributed into the experimental bottles. Initial headspace samples and initial samples for biomass measurements were taken before the experiment began. For trials conducted indoors, cultures were grown under an LED light source (custom solar spectrum mimicking light from G2V Optics, Edmonton Alberta Canada) for the number of hours outlined in Table 1. The light intensity was measured using a LI-180 spectrometer (LI-COR Biosciences, Lincoln, Nebraska, USA). For experiments conducted with sunlight (greenhouse or direct), light intensity was logged every 15 minutes using a LI-180 spectrometer (LI-COR Biosciences, Lincoln, Nebraska, USA). Light intensity, measured in μmol photons/m^2/s, was normalized for bottle area and for day length.

At the end of the experiment bottle pressure was measured, headspace samples were collected via needle through the bottle septum and stored in exetainers, and 150 mL of culture was centrifuged for measurements of biomass weight. Biomass samples were freeze dried or dried in an oven at 70°C until all liquid had evaporated and then weighed to determine the dry biomass weight.

Oxygen Measurements

Oxygen content in the headspace of culture bottles was measured using a 7890B Gas Chromatograph (Agilent Technologies, Santa Clara, California, US) with a thermal conductivity detector (TCD). 5 mL of headspace sample was injected into the instrument and the following protocol was run. Briefly, the instrument operated under the following parameters: valve temperature: 125°C; oven temperature: 105°C; post-run at oven temperature of 50°C for 0 min. Helium was used as a carrying gas at 21 mL/min. A 6′ × 1/8″ Hayesep N (80/100 mesh) column and an 8′ × 1/8″ MS5A (60/80 mesh) column were used to separate CO_2, N_2 and O_2.

To calculate the change in oxygen production, initial oxygen concentration was subtracted from final oxygen concentration. Moles of oxygen were calculated using the ideal gas law:

$$\mathbf{(1)}\quad PV = nRT$$

Where R = 0.08206 L atm $mol^{-1}K^{-1}$, and T is measured temperature (K). The increase in pressure was measured using a Leo3 manometer (Keller AG, Winterthur, Switzerland), and volume was determined from headspace volume and the gas fraction. Oxygen production was normalized for headspace volume, culture volume, hours of light, and initial dry biomass concentration in order to compare all experiments.

Fluorometry measurements

Fluorometric measurements to determine the cyanobacteria photochemistry were conducted using a Fluorcam FC 800-C (Photon System Instruments, Czech Republic) as described previously in Ataeian *et al.* (2019)[18], on 15 mL of cyanobacteria culture placed in a petri dish (Supplementary Figure 4).

Light attenuation measurements

The effect of light attenuation on cultures of different densities was measured using a Li-250A light meter (LI-COR Biosciences, Lincoln, Nebraska, USA) with a submersible spherical light probe. Measurements of light intensity were made at increasing depths below the culture surface until the light intensity reached less than 100 µmol photons/m^2/s (Supplementary Figure 6). Three, 10-second averages of light intensity were used for each measurement. Attenuation with and without a light filter was measured.

Fabrication of light filter

The light filters were fabricated by slot-die coating $tPDI_2N$-EH (PDI) solutions onto PET substrates in air followed by layering a plastic UV-blocking sheet onto the organic layer and finally encapsulation using 3M lamination sheets. Solutions were prepared at 2 mg/mL, 5 mg/mL, and 10 mg/mL for LF-1, LF-2, LF-3, respectively. The solvent used was *o*-xylene. The polymer styrene-butadiene-styrene (SBS, donated by Professor Martin Jasso at the University of Calgary) was used as an additive (20 mg/mL) to increased solution viscosity allowing for uniform and reproducible coatings. Solutions were slot-die coated (FOM Technologies compact sheet coater) at room temperature in air onto PET (gloss waterproof inkjet film, product code 7561011 from Printing Supplies Direct) sheets with a total dimension of 10 x 30 cm (Supplementary Figure 1). A 150 mm slot-die head with 100 mm shim was used with a flow rate of 120 µL/min and coating speed (substrate moving rate) of 3.5 cm/min. Sheets were then cut into three 10 x 10 cm pieces. A UV-barrier plastic film (Edmund Optics, item # 39426) treated with an anti-static roller (Teknek contact cleaning hand roller) was cut to size and placed onto the PDI film. A thermal lamination plastic film (3M Scotch, TP3854-100-C) treated with an anti-static roller was cut to size and placed on the bottom and top of stack. The entire stack was then pushed through a thermal laminator (Scotch, serial number 17092505289, model TL902-C) to yield the final light filters used in this study.

Fabrication of OPV devices

All OPV devices were fabricated and tested as per reported procedure[33]. To control the illumination intensity (i.e. testing under 0.79, 0.63 and 0.28 sun conditions) neutral density filters were used in between the light source and OPV device (ThorLabs, items NE201B, NE202B and NE206B).

Theoretical calculations and modelling

The photosynthetic productivity model (eqn. 2) was based on the simplified light inhibition model[28,55]. It is a function of light intensity at a defined depth in the system and is dependent on two empirical parameters but does not account for the effects of nutrient concentrations or temperature.

(2)

$$P(l) = \frac{I(l)}{K_1 + K_2 I(l)^2}$$

Where, $P(l)$ is the productivity in μmol O_2/(g dry biomass·s) at depth l in cm, $I(l)$is the light intensity in μmol photons/(m^2·s) at depth l, and K_1 and K_2 are constants in (μmol photons · g dry biomass)/(μmol O_2 ·m^2) and (g dry biomass · m^2·s^2)/(μmol photons · μmol O_2) respectively.

Light intensity at depth was modeled using the Beer-Lambert Law (eqn 3). A constant (ω) was added to the Beer-Lambert law to account for the fraction of incident light not reflected by the fluid. This constant was assumed to be invariable with scale.

(3)

$$I(l) = \omega I \exp(-\varepsilon c l)$$

Where, I is the incident light intensity in μmol photons/(m^2·s), ω is the transmitted fraction of light, ε is the mass extinction coefficient in cm^2/(g dry biomass), and c is the algal concentration in g dry biomass)/cm^3.

The Beer-Lambert law was fit to empirical data generated from light attenuation measurements giving a mass extinction coefficient (ε) of 750.6 cm^2/(g dry biomass) and a transmitted fraction (ω) of 0.63576.

Equations 2 and 3 were combined to give the full algal productivity model (eqn. 4) as a function of depth.

(4)

$$P(l) = \frac{\omega I \exp(-\varepsilon c l)}{K_1 + K_2 \omega^2 I^2 \exp(-\varepsilon c l)^2}$$

Equation 4 can be integrated across the algal mass of the system to give the productivity of the full pond volume (eqn. 5).

(5)

$$P_t = \frac{A}{\epsilon\sqrt{K_1 K_2}}\left[\tan^{-1}\left(\sqrt{\frac{K_1}{K_2}}\frac{\exp(\epsilon c H)}{\omega I}\right) - \tan^{-1}\left(\sqrt{\frac{K_1}{K_2}}\frac{1}{\omega I}\right)\right]$$

Where P_t is the total productivity of the system in μmol O_2/(g dry biomass·s), and A is the area in cm^2. The values of K_1 and K_2 were determined by fitting the integrated model to empirical productivity data collected at various algal concentrations. The values of K_1 and K_2 were determined to be 199.7 μmol photons · g dry biomass)/(μmol $O_2 \cdot m^2$) and 0.002564 (g dry biomass · $m^2 \cdot s^2$)/(μmol photons · μmol O_2) respectively. Equation five can be normalized (eqn. 6) to a per unit mass basis by dividing equation 5 by the total mass of the system, cV.

(6)

$$P = \frac{1}{\epsilon c H\sqrt{K_1 K_2}}\left[\tan^{-1}\left(\sqrt{\frac{K_1}{K_2}}\frac{\exp(\epsilon c H)}{\omega I}\right) - \tan^{-1}\left(\sqrt{\frac{K_1}{K_2}}\frac{1}{\omega I}\right)\right]$$

Where P is the normalized productivity in µmol O_2/(g dry biomass·s)

Normalized photosynthetic productivity data (µmol O_2/g dry biomass/s) was converted to areal productivity (g dry biomass/m^2/12 hour day) assuming a 1:1 ratio of moles of oxygen produced to moles of biomass produced, which represents the theoretical maximum for a biomass accumulation efficiency value[6]. The molecular weight of biomass was assumed to be 24.6 g/mol (molecular weight for biomass formula: $C_1H_{1.8}O_{0.5}N_{0.2}$)

Power production analysis

Using the modelled relationship between light and biomass production, we aimed to address the feasibility of combining light filtration and the growth of the cyanobacterial consortium in a realistic scenario. To further explore this possibility, we assumed that the light filter tPDI$_2$N-EH was part of an optimized organic photovoltaic (OPV) device which would be used to generate electricity. To directly compare the power equivalent of biomass and electricity, we have calculated the calorific values (higher heating values, HHV) of the dry biomass. HHV defines the energy content of the fuel, which aids in the performance evaluation of the fuels. Numerous correlations for calculation of HHV from the elemental composition of biomass are available in the literature. We have used the average HHV outputs of the two most known formulas for biomass and solid fuels which gave a value of 15.7 MJ/kg[35,36]:

HHV = 0.3491C + 1.1783H + 0.1005S – 0.1034O – 0.0151N – 0.0211A (MJ/kg)[36]

HHV = 0.33C + 1.42H – 0.15O - 14.5 N (MJ/Kg)[35]

C, H, O, N, and S represent carbon, hydrogen, oxygen, nitrogen, and sulfur contents of algae expressed in mass percentages on a dry basis. Based on mass percentage: 40% C, 6% H, 45% O, 0.63% N, 0.5% S[35,36].

Solar radiation data for the four locations, Calgary Alberta Canada (51.04° N, 114.07° W), Honolulu Hawaii USA (21.31°N, 157.86° W), Phoenix Arizona USA (33.45° N, 112.07° W), and Chicago Illinois USA (41.88° N, 87.63° W), were obtained from the National Solar Radiation Database[56]. Global Horizontal Irradiance (GHI) values were retrieved, and monthly averages were calculated for each location over the years of 2014-2018.

A power conversion efficiency (PCE) of 4.2% for an optimized model OPV device containing a PTQ10/PDI active layer was measured experimentally, and this was used to calculate the OPV power output (Supplementary Table 1). The optimized OPV device allowed 40% light transmission. This PCE value was used because it corresponded to the experimental light level that was closest to the historical radiation data (Supplementary Table 1).

Photosynthetically active radiation (PAR), which is the wavelength range used in photosynthesis, was calculated from the monthly averages. Watts were converted to µmol photons via a conversion factor of 4.6 µmol photons/m^2/s = 1 W/m^2 for natural sunlight[57]. PAR radiation was assumed to account for roughly 45% of total spectrum irradiation, and this was also factored into calculations[7]. Additionally, light intensity was normalized per month for average day length in each of the respective cities. These normalized irradiance values were used to calculate an average monthly productivity with and without an optimized OPV device of 40% transmission, given a pond size of 100m^2, a depth of 20 cm, and a dry biomass concentration of either 0.5 g/L, or 0.1 g/L.

References

1. Davis, R. *et al.* Process design and economics for the production of algal biomass: Algal biomass production in open pond systems and processing through dewatering for downstream conversion. *NREL TP-5100-64772* (2016).
2. Brennan, L. & Owende, P. Biofuels from microalgae – A review of technologies for production, processing, and extractions of biofuels and co-products. *Renew. Sustain. Energy Rev*. **14**, 557-577 (2010).
3. Laurens, L., M., L., Chen-Glasser, M. & McMillan, J. D. A perspective on renewable bioenergy from photosynthetic algae as feedstock for biofuels and bioproducts. *Algal Res*. **24**, 261-264 (2017).
4. Quinn, J., C. & Davis, R. The potentials and challenges of algae based biofuels: A review of the techno-economic, life cycle, and resource assessment modeling. *Bioresour. Technol*. **184**, 444-452 (2015).
5. Bolton, J. & Hall, D. The maximum efficiency of photosynthesis. *Photochem. Photobiol*. **53**, 545-548 (1991).
6. Weyer, K., Bush, D., Darzins, A. & Wilson, B. Theoretical maximum algal oil production. *Bioenerg. Res.* **3**, 204-213 (2010).
7. Ooms, M.D., Dinh, C.T., Sargent, E.H. & Sinton, D. Photon management for augmented photosynthesis. *Nat. Commun*. **1**, 12699 (2016).
8. Goldman, J. Outdoor algal mass cultures – II. Photosynthetic yield limitations. *Water Res*. **13**, 119-136 (1979).
9. Luimstra, V. *et al*. Blue light reduces photosynthetic efficiency of cyanobacteria through an imbalance between photosystems I and II. *Photosyn. Res*. **138**, 177-189 (2018).
10. Detweiler, A.M. *et al.* Evaluation of wavelength selective photovoltaic panels on microalgae growth and photosynthetic efficiency. *Algal Res*. **9**, 170-177 (2015).

11. Wondraczek, L. *et al.* Solar spectral conversion for improving the photosynthetic activity in algae reactors. *Nat. Commun*. **4**, 2047 (2013).
12. Sharp, C. *et al*. Robust, high-productivity phototrophic carbon capture at high pH and alkalinity using natural microbial communities. *Biotechnol. Biofuels*. **10**, 84 (2017).
13. Melis, A. Solar energy conversion efficiencies in photosynthesis: Minimizing the chlorophyll antennae to maximize efficiency. *Plant Sci*. **177**, 272-280 (2009).
14. Cui, Y. *et al.* Wide-gap non-fullerene acceptor enabling high-performance organic photovoltaic cells for indoor applications. *Nat. Energy*. **4**, 768-775 (2019).
15. Leo, K. Organic photovoltaics. *Nat. Rev. Mater*. **1**, 16056. (2016).
16. Su, Y-W., Lan, S-C. & Wei, K-H. Organic photovoltaics. *Mater. Today*. **15**, 554-562 (2012).
17. Zorz, J.K. *et al*. A shared core microbiome in soda lakes separated by large distances. *Nat. Commun.* **10**, 4230 (2019).
18. Ataeian, M. *et al*. Direct capture and conversion of CO_2 from air by growing a cyanobacterial consortium at pH up to 11.2. *Biotechnol. Bioeng*. **116**, 1604-1611 (2019).
19. Hendsbee A.D. *et al*. Synthesis, self-assembly, and solar cell performance of N-annulated perylene diimide non-fullerene acceptors. **28**, 7098-7109 (2016).
20. Dayneko, S., Hendsbee, A. & Welch, G.C. Combining facile synthetic methods with greener processing for efficient polymer-perylene diimide based organic solar cells. *Small methods*. **2**, 1800081 (2018).
21. Kozma, E. & Catellani, M. Perylene diimides based materials for organic solar cells. *Dyes Pigm.* **98**, 160-179 (2013).
22. Wurthner, F. *et al*. Perylene bisimide dye assemblies as archetype functional supramoleculuar materials. *Chem. Rev*. **116**, 962-1052 (2016).
23. Li, M., Yin, H. & Sun, G-Y. PDI derivatives with functional active position as non-fullerene small molecule acceptors in organic solar cells: From different core linker to various conformation. *Mater. Today*. **21**, 100799 (2020).

24. Danyeko, S., Pahlevani, M. & Welch, G.C. Indoor photovoltaics: Photoactive material selection, greener ink formulations, and slot-die coated active layers. *ACS Appl. Mater. Interfaces*. **11**, 46017-46025 (2019).
25. Tintori, F., Laventure, A. & Welch, G.C. Perylene diimide based organic photovoltaics with slot-die coated active layers from halogen-free solvents in air at room temperature. *ACS Appl. Mater. Inter*. **11**, 39010-39017 (2019).
26. Farahat, M. *et al*. Slot-die-coated ternary organic photovoltaics for indoor light recycling. *ACS Appl. Mater. Interfaces*. **12**, 43684-43693. (2020).
27. Campbell, D., Hurry, V., Clarke, A.K., Gustafsson, P. & Oouist, G. Chlorophyll fluorescence analysis of cyanobacterial photosynthesis and acclimation. *Microbiol. Mol. Biol. Rev*. **62**, 667-683 (1998).
28. Bechet, Q., Shilton, A. & Guieysse, B. Modeling the effects of light and temperature on algae growth: state of the art and critical assessment for productivity prediction during outdoor cultivation. *Biotechnol. Adv*. **31**, 1648-63 (2013).
29. Vadlamani, A., Pendyala, B., Viamajala, S. & Varanasi S. High productivity cultivation of microalgae without concentrated CO_2 input. *ACS Sustain. Chem. Eng.* **7**, 1933-1943 (2019).
30. Angmo, D., & Krebs, F.C. Over 2 years of outdoor operational and storage stability of ITO-Free, fully roll-to-roll fabricated polymer solar cell modules. *Energy Technol*. **3**, 774-783 (2015).
31. Sun, C. *et al.* A low cost and high performance polymer donor material for polymer solar cells. *Nat. Comm.* **9**, 743 (2018).
32. Huang, H. *et al.* Green solvent-processed organic solar cells based on a low cost polymer donor and a small molecule acceptor. *J. Mater. Chem. C.* **8**, 7718-7724 (2020).
33. Tintori, F., Laventure, A., Koenig, J.D.B. & Welch, G.C. High open-circuit voltage roll-to-roll compatible processed organic photovoltaics. *J. Mater. Chem. C*. Advance Article. (2020).
34. Wu, Y. *et al.* Rationally pairing photoactive materials for high-performance polymer solar cells with efficiency of 16.53%. *Sci. China Chem.* **63**, 265-271 (2020).

35. Demirbas, A. Calculation of higher heating values of biomass fuels. *Fuel*. **76**, 431-434 (1997).
36. Channiwala, S.A. & Parikh, P.P. A unified correlation for estimating HHV of solid, liquid and gaseous fuels. *Fuel*. **81**, 1051-1063 (2002).
37. Nwoba, E., Parlevliet, D., Laird, D., Alameh, K. & Moheimani, N. Light management technologies for increasing algal photobioreactor efficiency. *Algal Res*. **39**, 101433 (2019).
38. Li, Y. *et al*. High efficiency near-infrared and semitransparent non-fullerene acceptor organic photovoltaic cells. *J. Am. Chem. Soc*. **139**, 17114-17119 (2017).
39. Cheng, P., Li, G., Zhan, X. & Yang, Y. Next-generation organic photovoltaics based on non-fullerene acceptors. *Nat. Photonics*. **12**, 131-142 (2018).
40. Hou, J., Inganas, O., Friend, R.H. & Gao, F. Organic solar cells based on non-fullerene acceptors. *Nat. Mater*. **17,** 119-128 (2018).
41. Zhang, J., Tan, H.S., Guo, X., Facchetti, A. & Yan, H. Material insights and challenges for non-fullerene organic solar cells based on small molecular acceptors. *Nat. Energy*. **3**, 720-731 (2018).
42. Liu, Y. *et al*. Unraveling sunlight by transparent organic semiconductors toward photovoltaic and photosynthesis. *ACS. Nano*. **13**,1071-1077 (2019).
43. Mohsenpour, S.F., Richards, B. & Willoughby, N. Spectral conversion of light for enhanced microalgae growth rates and photosynthetic pigment production. *Bioresour. Technol.* **125**, 75-81 (2012).
44. Helgesen, M., Sondergaard, R. & Krebs, F.C. Advanced materials and processes for polymer solar cell devices. *J. Mater. Chem*. **20**, 36-60 (2010).
45. Krebs, F.C., Fyenbo, J. & Jorgensen, M. Product integration of compact roll-to-roll processed polymer solar cell modules: methods and manufacture using flexographic printing, slot-die coating and rotary screen printing. *J. Mater. Chem*. **20**, 8994-9001 (2010).
46. Zhou, Y. *et al.* Recyclable organic solar cells on cellulose nanocrystal substrates. *Sci. Rep*. **3**, 1536 (2013).

47. Emmott, C.J.M. *et al.* Organic photovoltaic greenhouses: a unique application for semi-transparent PV? Energy Environ. Sci., **8**, 1317 (2015).
48. Zhang, J., Zhu, L. & Wei, Z. Toward over 15% power conversion efficiency for organic solar cells: Current status and perspectives. *Small Methods*. **1**, 1700258 (2017).
49. Xue, Q., Xia, R., Brabec, C.J. & Yip, H-L. Recent advances in semi-transparent polymer and perovskite solar cells for power generating window applications. *Energy Environ. Sci*. **11**, 1688-1709 (2018).
50. Xie, Y. *et al*. Highly transparent organic solar cells with all-near-infrared photoactive materials. *Small Methods*. **3**,1900424 (2019).
51. Ravishankar, E. *et al*. Achieving net zero energy greenhouses by integrating semitransparent organic solar cells. *Joule*. **4**, 490-506 (2020).
52. Hollingsworth, J.A., Ravishankar, E., O'Connor, B., Johnson, J.X. & DeCarolis, J.F. Environmental and economic impacts of solar-powered integrated greenhouses. *J. Ind. Ecol*. **24**, 234-247. (2019).
53. Loik, M. *et al.* Wavelength-selective solar photovoltaic systems: powering greenhouses for plant growth at the food-energy-water nexus. *Earths Future*. **5**, 1044-1053 (2017).
54. Michael, C., del Ninno, M., Gross, M. & Wen, Z. Use of wavelength-selective optical light filters for enhanced microalgal growth in different algal cultivation systems. *Bioresour. Technol*. **179**, 473-482 (2015).
55. Lee, H., Erickson, L. & Yang, S. Kinetics and bioenergetics of light-limited photoautotrophic growth of *Spirulina platensis*. *Biotechnol. Bioeng*. **29**, 832-843 (1987).
56. Sengupta, M. *et al*. The National Solar Radiation Data Base (NSRDB). *Renew. Sustain. Energy Rev*. **89**, 51-60 (2018).
57. Thimijan, R.W. & Heins, R.D. Photometric, radiometric, and quantum light units of measure: A review of procedures for interconversion. *Hortic. Sci.* **18**, 818-820 (1983).

58. Bristow, N., & Kettle, J. Outdoor organic photovoltaic module characteristics: Benchmarking against other PV technologies for performance, calculation of Ross coefficient and outdoor stability monitoring. *Sol. Energy Mater. Sol. Cells.* **175**, 52-59 (2018).
59. Huang, K-M. *et al.* Highly efficient and stable organic solar cell modules processed by blade coating with 5.6% module efficiency and active area of 216 cm^2. **27**, 264-274 (2019).

Acknowledgements

We would like to thank Jianwei Chen and Breda Novotnik for help with method development and analysis with the GC. We would like to thank Timber Gillis for help in performing preliminary experiments, and Daniel Gittins for providing valuable feedback on the manuscript. This work was supported by the Natural Sciences and Engineering Research Council (NSERC), Canada Foundation for Innovation (CFI), Canada First Research Excellence Fund (CFREF), Western Economic Diversification, Alberta Innovates, the Government of Alberta, and the University of Calgary.

Author Contributions

JZ planned and performed experiments, analyzed experimental data, and wrote the manuscript. WR created the productivity model and provided feedback on the manuscript. MH performed light attenuation experiments and provided feedback on the model and the manuscript, AV provided feedback on the manuscript and productivity model, and helped to perform experiments. AL and EC carried out the light filter and OPV work. AA performed the power generation analysis and provided feedback on the manuscript. JB, GW, and MS conceived the study, and provided feedback on the model, analysis, and manuscript.

Competing interests

The authors declare no competing interests.

Figure Legends

Figure 1. Details of light filters used in experiments with the cyanobacterial consortium. a) Chemical structure of the organic dye tPDI$_2$N-EH (PDI). b) Representation of the slot-die coating process used to manufacture the light filters. c) Schematic of the light filter layers. d) Photos of the light filters used for experiments. e) Transmission spectra of light filters

Figure 2. Ratio of normalized photosynthetic oxygen production of samples grown with light filters to samples grown without filters for the same experimental condition. Individual sample points are overlaid. The dashed line highlights a fold difference of 1, above which the use of light filters becomes advantageous. The x-axis shows incident light intensity, which refers to the light intensity prior to light filtration by the filters. LF-1: filter with 70% transmission, LF-2: filter with 50% transmission, LF-3: filter with 30% transmission.

Figure 3. Predicted photosynthetic productivity using the photosynthetic growth model. a) Integrated model (purple) with experimental data (light green). Integrated contour plots of areal productivity (g/m^2/12 hour day) as a function of light intensity (x axis) and filter transmission (y axis) in a pond of 20 cm depth with 0.1 g/L (b), and 0.5 g/L (c) dry biomass concentration. The colour at each intersection of filter transmission and light intensity corresponds to the predicted areal photosynthetic growth under those combined conditions.

Figure 4. Use of the photosynthetic productivity model to estimate power output from a combination of photosynthesis and light filtering by a PDI-based OPV at four North American locations. (a) The average monthly solar radiation from 2014-2018, in W/m^2 in the four cities chosen, normalized for average monthly day length. (b) The ratio of power produced when the algae and an OPV device are combined compared to the power produced by the algae alone. The line shows the average power ratio of a culture at 0.1 g/L and a culture at 0.5 g/L. c) The average monthly estimated power production of the algae and OPV technologies alone and the algae and OPV technologies combined. The data presented here are the average monthly projections for Phoenix, and represent the average power produced between 0.1 and 0.5 g/L cultures. Supplementary Figure 7 shows data for all four cities at 0.1 g/L and 0.5 g/L culture density. Algal growth was derived from the photosynthetic productivity model and predicted OPV power was calculated using a power conversion efficiency (PCE) of 4.2% (Supplementary Table 1). This power conversion efficiency is appropriate for OPV modules[58,59].

Figure 5. Solar conversion efficiencies and algal growth. a) Average annual photosynthetic efficiency of algae grown with OPV light filtration (light green), and without (dark green). b) Average annual power production of algae grown with OPV light filtration (light green), and without (dark green). c) Solar conversion efficiency of algal photosynthesis (dark green), OPV (yellow), and both technologies combined (light green). Values displayed are the average between 0.1 and 0.5 g/L cultures.

Figures

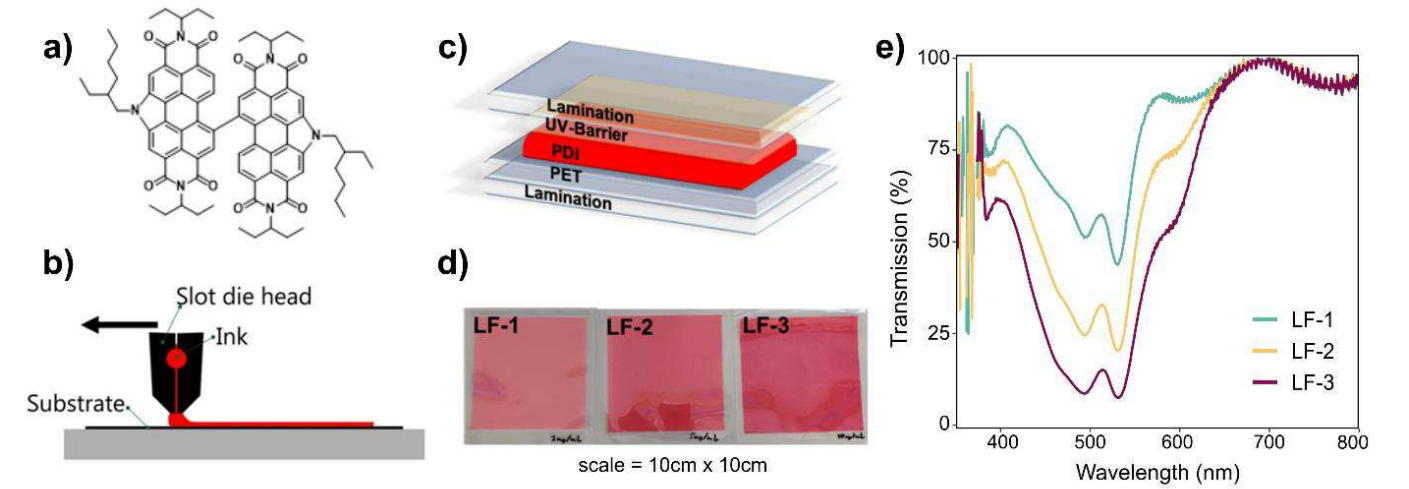

Figure 1. Details of light filters used in experiments with the cyanobacterial consortium. a) Chemical structure of the organic dye $tPDI_2N$-EH (PDI). b) Representation of the slot-die coating process used to manufacture the light filters. c) Schematic of the light filter layers. d) Digital pictures of the light filters used for experiments. e) Transmission spectra of light filters.

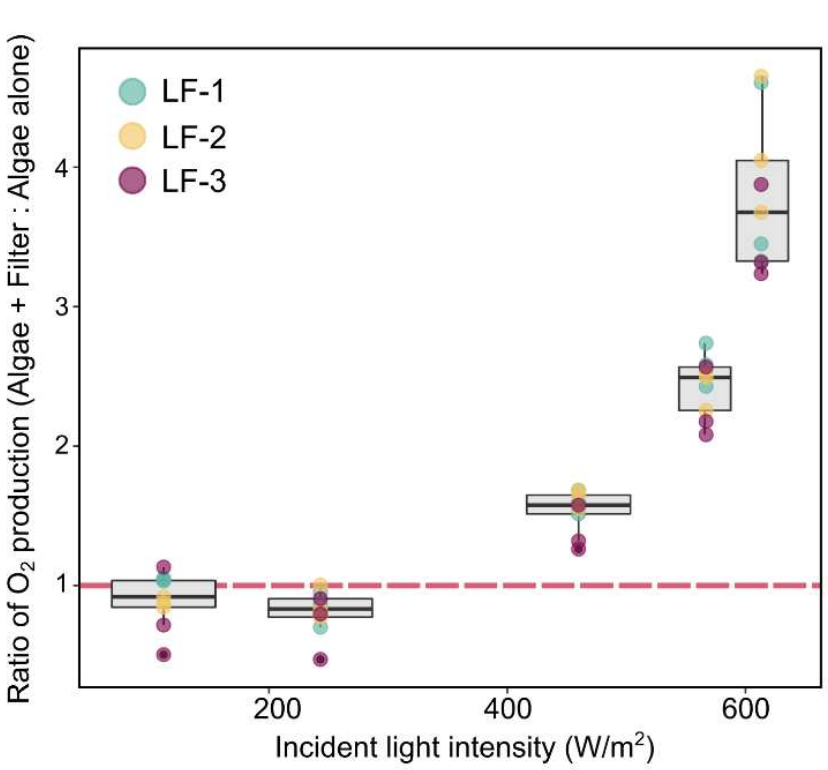

615

616

617 **Figure 2.** Ratios of normalized photosynthetic oxygen production of samples grown with light filters to
618 samples grown without filters for the same experimental condition. Individual sample points are overlaid.
619 The dashed line highlights a fold difference of 1, above which the use of light filters becomes
620 advantageous. The x-axis shows incident light intensity, indicating, the light intensity prior to light
621 filtration by the filters. LF-1: filter with 70% transmission, LF-2: filter with 50% transmission, LF-3:
622 filter with 30% transmission.

623

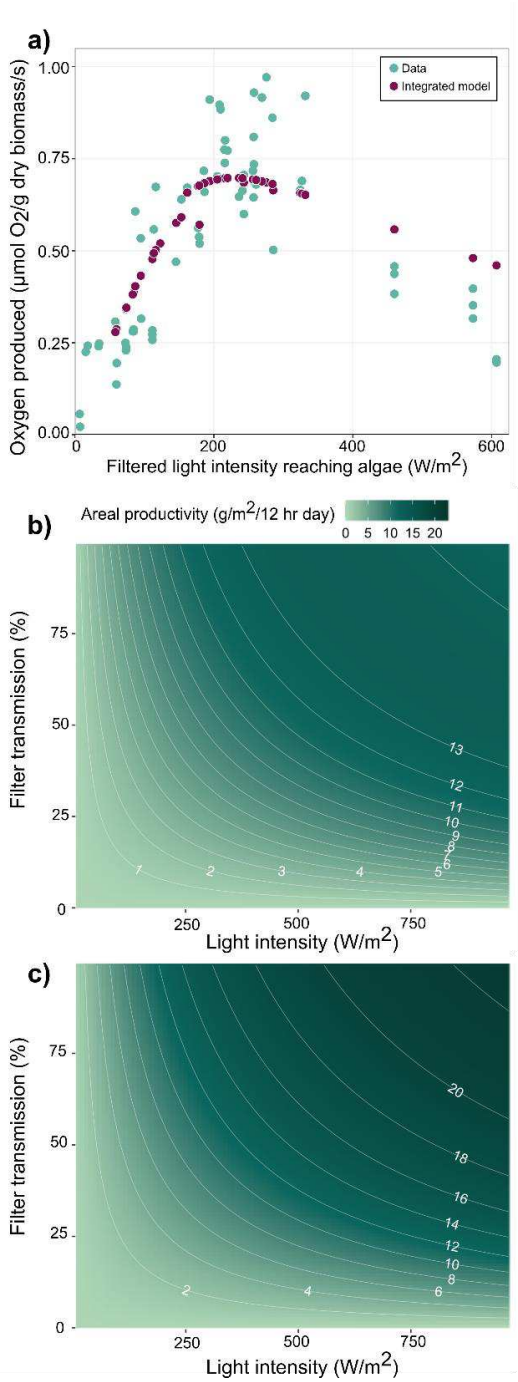

Figure 3. Predicted photosynthetic productivity using the photosynthetic growth model. a) Integrated model (purple) with experimental data (light green). Integrated contour plots of areal productivity as a function of light intensity (x-axis) and filter transmission (y-axis) in a pond of 20 cm depth with 0.1 g/L (b), and 0.5 g/L (c) dry biomass concentration. The colour at each intersection of filter transmission and light intensity corresponds to the predicted areal photosynthetic growth under those combined conditions.

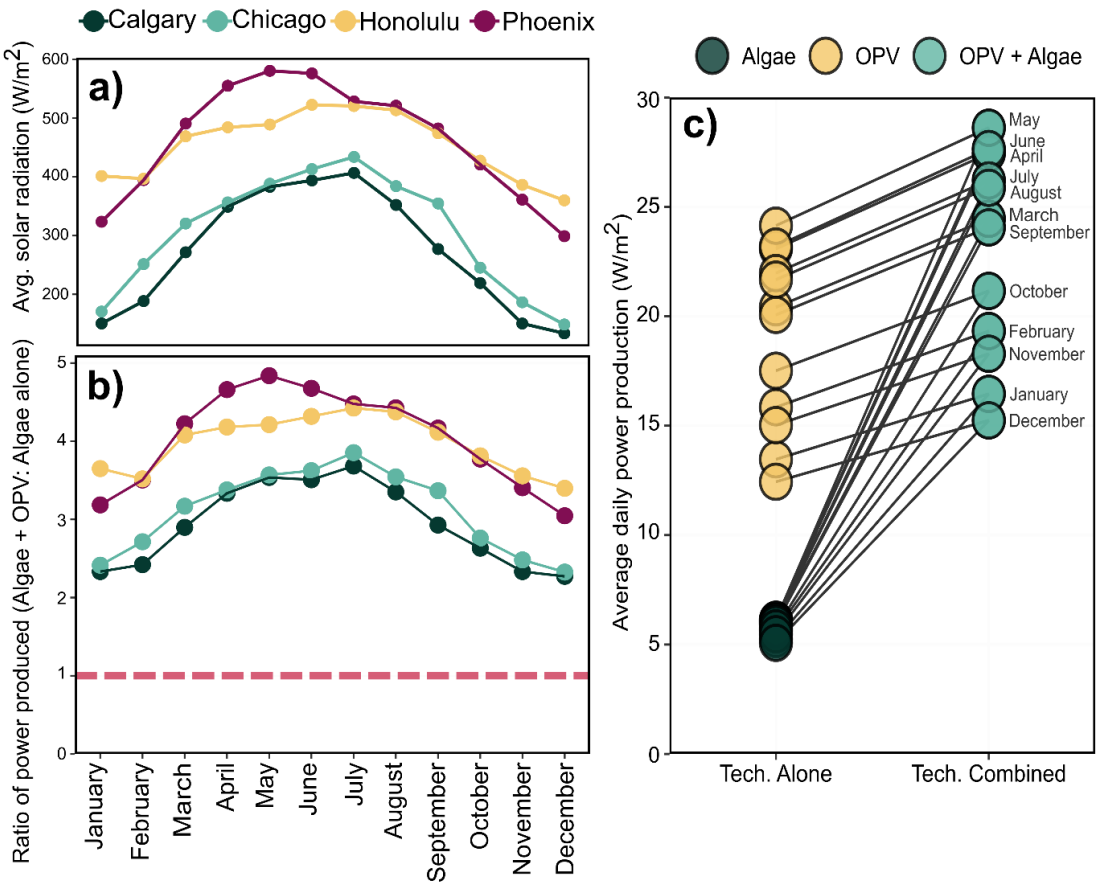

Figure 4. Photosynthetic productivity model power output estimates from a combination of photosynthesis and light filtering by a PDI-based OPV at four North American locations. (a) The average monthly solar radiation from 2014-2018, in W/m^2 in the four cities chosen, normalized for average monthly day length. (b) The ratio of power produced when the algae and an OPV device are combined compared to the power produced by the algae alone. The line shows the average power ratio of a culture at 0.1 g/L and a culture at 0.5 g/L. (c) The average monthly estimated power production of the algae and OPV technologies alone and the algae and OPV technologies combined. The data presented here are the average monthly projections for Phoenix, and represent the average power produced between 0.1 and 0.5 g/L cultures. Supplementary Figure 7 shows data for all four cities at 0.1 g/L and 0.5 g/L culture density. Algal growth was derived from the photosynthetic productivity model and predicted OPV power was calculated using a power conversion efficiency (PCE) of 4.2% (Supplementary Table 1). This power conversion efficiency is appropriate for OPV modules[58,59].

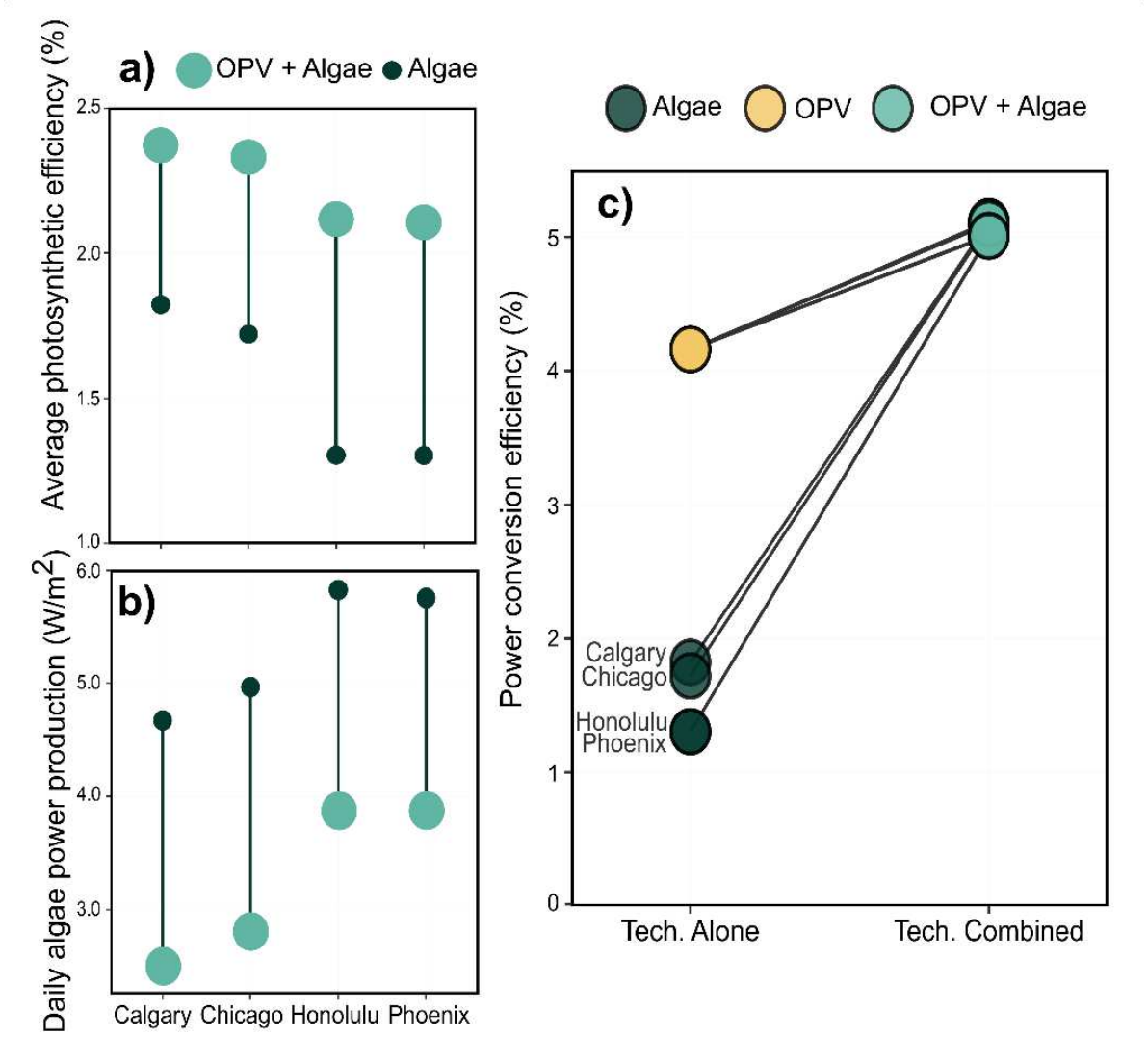

644

645 **Figure 5.** Solar conversion efficiencies and algal growth. a) Average annual photosynthetic efficiency of
646 algae grown with OPV light filtration (light green), and without (dark green). b) Average annual power
647 production of algae grown with OPV light filtration (light green), and without (dark green). c) Solar
648 conversion efficiency of algal photosynthesis (dark green), OPV (yellow), and both technologies
649 combined (light green). Values displayed are the average between 0.1 and 0.5 g/L cultures.

650

651

Tables

Table 1. Table of experimental conditions for data collected and used in model fitting and testing

Trial	Number of samples	Filters used	Light source	Bottle	Culture volume (mL)	Headspace (mL)	Initial conc. (dry) (g/L)	Hours of light	Model
1	2	No	G2V light	Cylindrical	120	39.5	0.35	16	Test
2	2	No	G2V light	Cylindrical	120	39.5	0.48	16	Test
3	2	No	G2V light	Cylindrical	120	39.5	0.68	16	Test
4	1	Yes	G2V light	Rectangular	217.5	72.5	0.38	16	Fit
5	1	No	G2V light	Rectangular	217.5	72.5	0.38	16	Fit
6	12	Yes	Sunlight – greenhouse	Rectangular	258	31.5	0.20	12	Fit
7	12	Yes	Sunlight – greenhouse	Rectangular	210	80	0.22	12	Fit
8	12	Yes	Sunlight – direct	Rectangular	210	80	0.06	10	Fit
9	12	Yes	Sunlight – direct	Rectangular	210	80	0.06	10	Fit
10	12	Yes	Sunlight – direct	Rectangular	210	80	0.065	10	Fit

List of Supplementary Tables and Figures

Supplementary Tables

Supplementary Figures

Figures

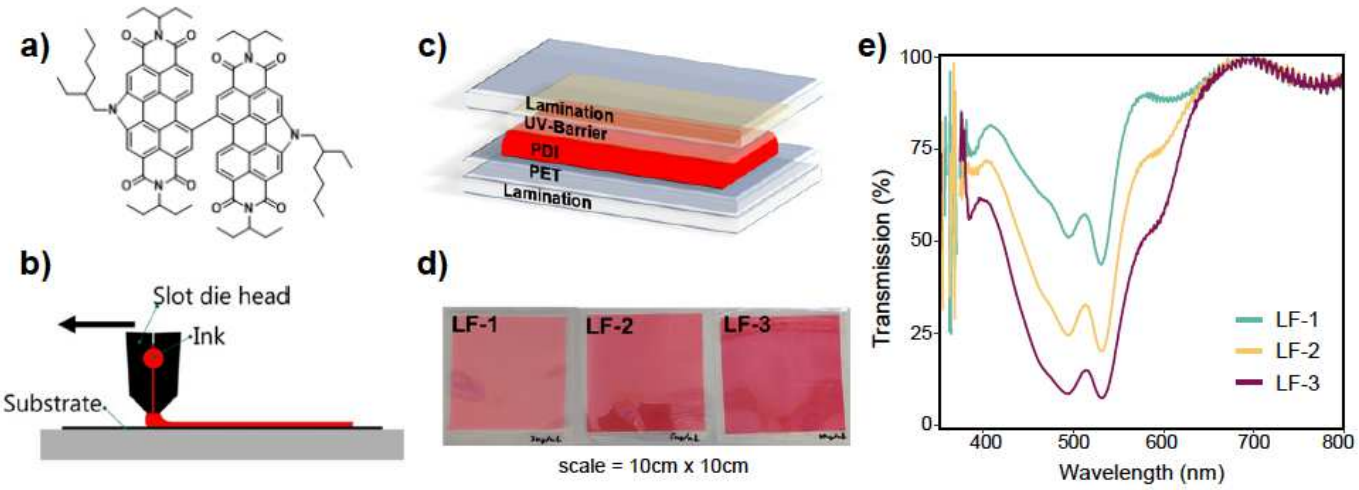

Figure 1

Details of light filters used in experiments with the cyanobacterial consortium. a) Chemical structure of the organic dye tPDI2N-EH (PDI). b) Representation of the slot-die coating process used to manufacture the light filters. c) Schematic of the light filter layers. d) Digital pictures of the light filters used for experiments. e) Transmission spectra of light filters.

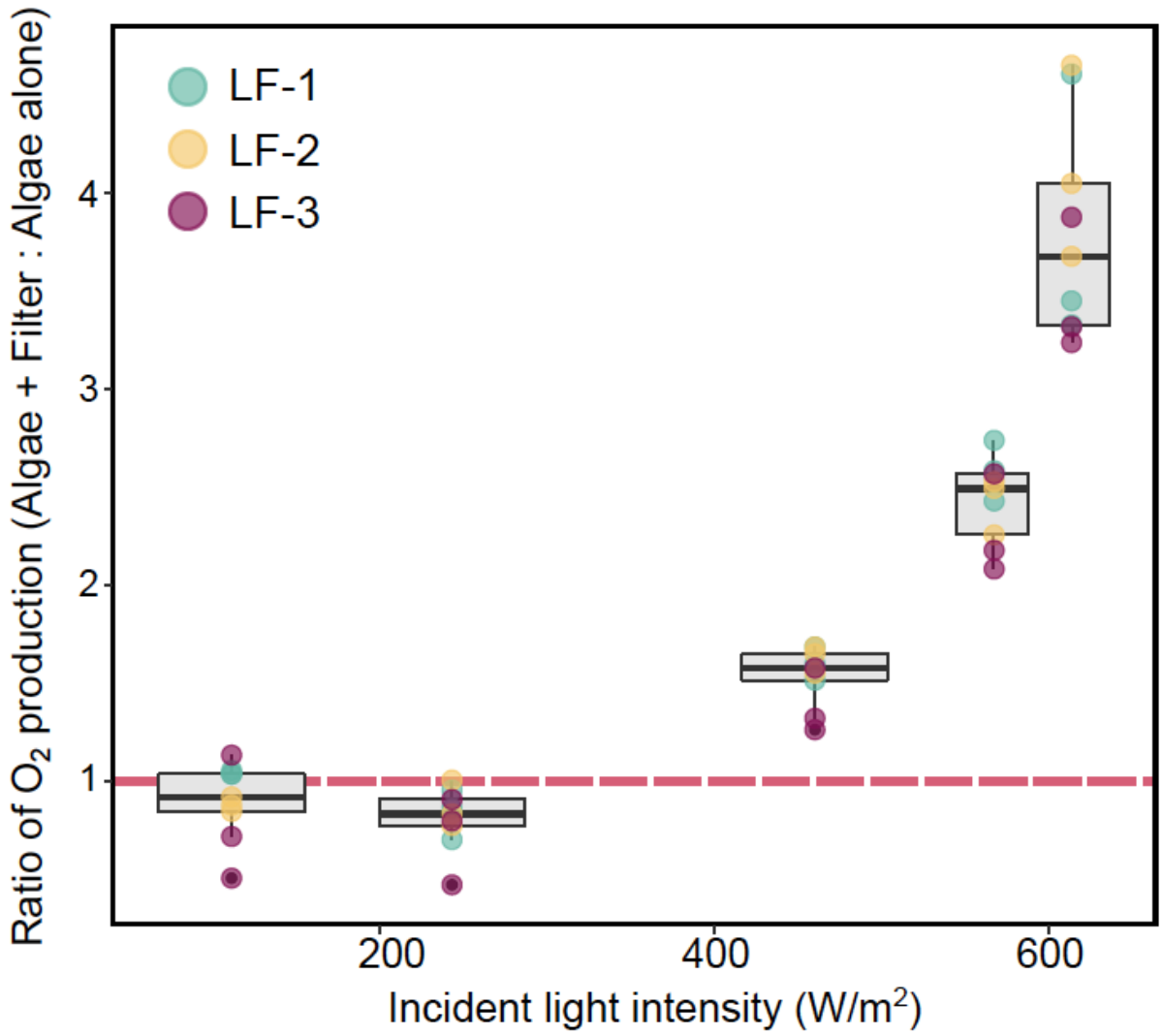

Figure 2

Ratios of normalized photosynthetic oxygen production of samples grown with light filters to samples grown without filters for the same experimental condition. Individual sample points are overlaid. The dashed line highlights a fold difference of 1, above which the use of light filters becomes advantageous. The x-axis shows incident light intensity, which refers to the light intensity prior to light filtration by the filters. LF-1: filter with 70% transmission, LF-2: filter with 50% transmission, LF-3: filter with 30% transmission.

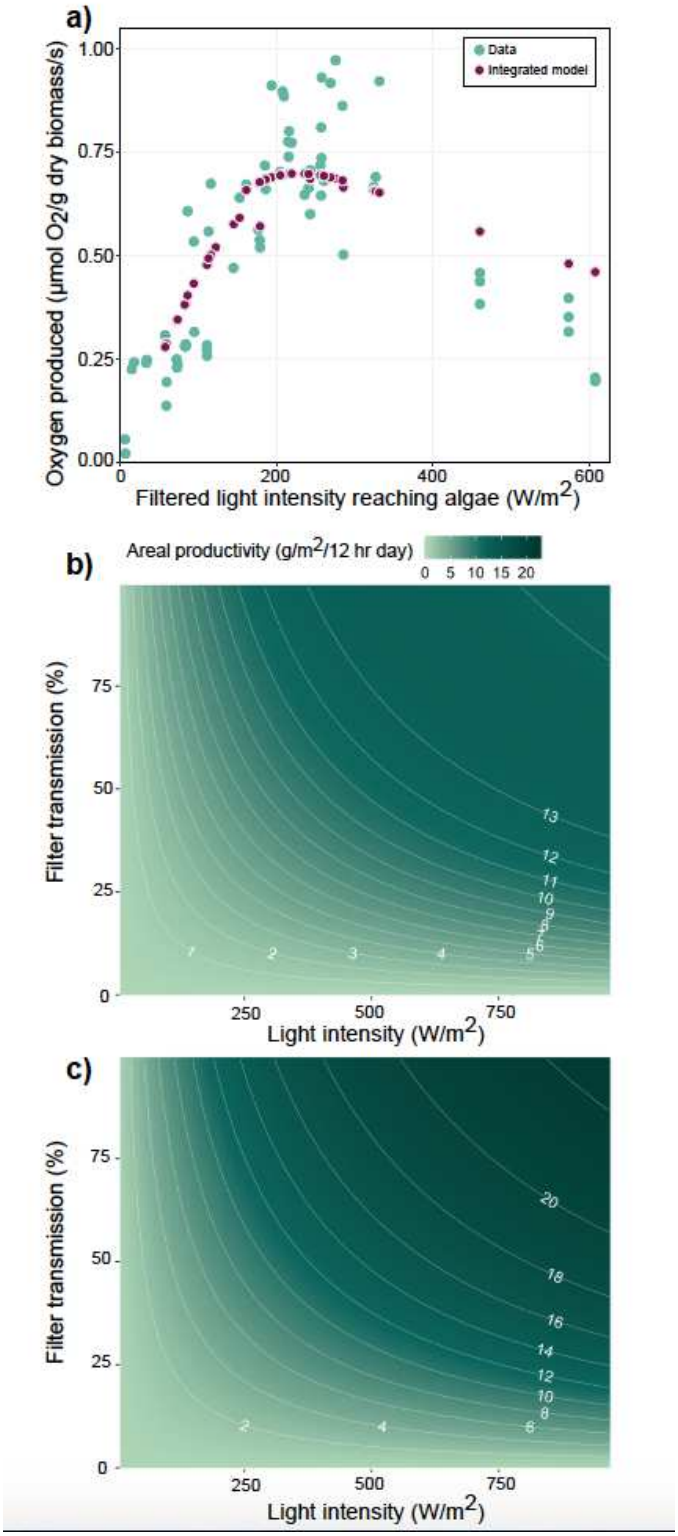

Figure 3

Predicted photosynthetic productivity using the photosynthetic growth model. a) Integrated model (purple) with experimental data (light green). Integrated contour plots of areal productivity (g/m2/12 hour day) as a function of light intensity (x axis) and filter transmission (y axis) in a pond of 20 cm depth with 0.1 g/L (b), and 0.5 g/L (c) dry biomass concentration. The colour at each intersection of filter

transmission and light intensity corresponds to the predicted areal photosynthetic growth under those combined conditions.

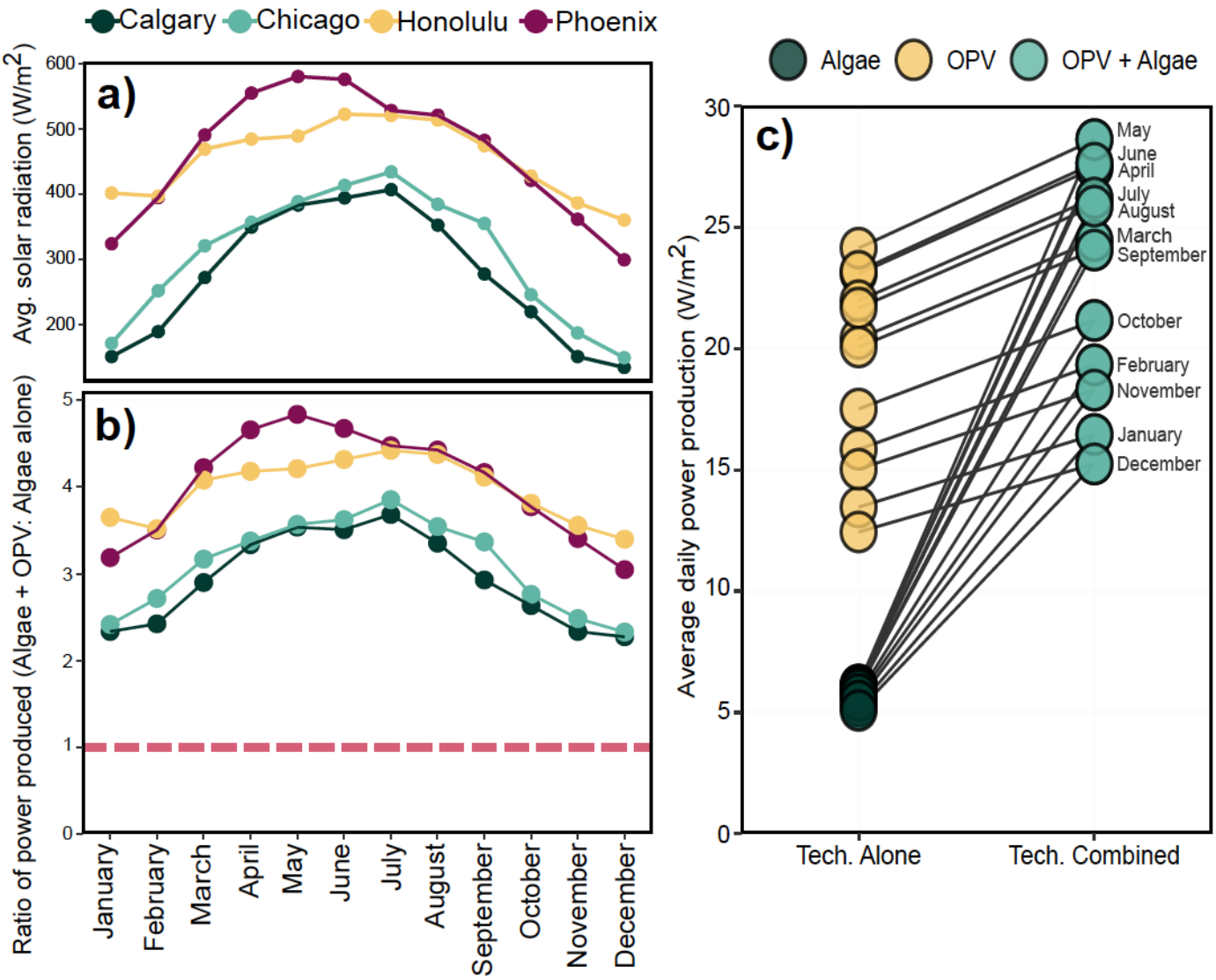

Figure 4

Photosynthetic productivity model power output estimates from a combination of photosynthesis and light filtering by a PDI-based OPV at four North American locations. (a) The average monthly solar radiation from 2014-2018, in W/m2 in the four cities chosen, normalized for average monthly day length. (b) The ratio of power produced when the algae and an OPV device are combined compared to the power produced by the algae alone. The line shows the average power ratio of a culture at 0.1 g/L and a culture at 0.5 g/L. c) The average monthly estimated power production of the algae and OPV technologies alone and the algae and OPV technologies combined. The data presented here are the average monthly projections for Phoenix, and represent the average power produced between 0.1 and 0.5 g/L cultures. Supplementary Figure 7 shows data for all four cities at 0.1 g/L and 0.5 g/L culture density. Algal growth was derived from the photosynthetic productivity model and predicted OPV power was calculated using a

power conversion efficiency of 4.2% (Supplementary Table 1). This power conversion efficiency is appropriate for OPV modules58,59.

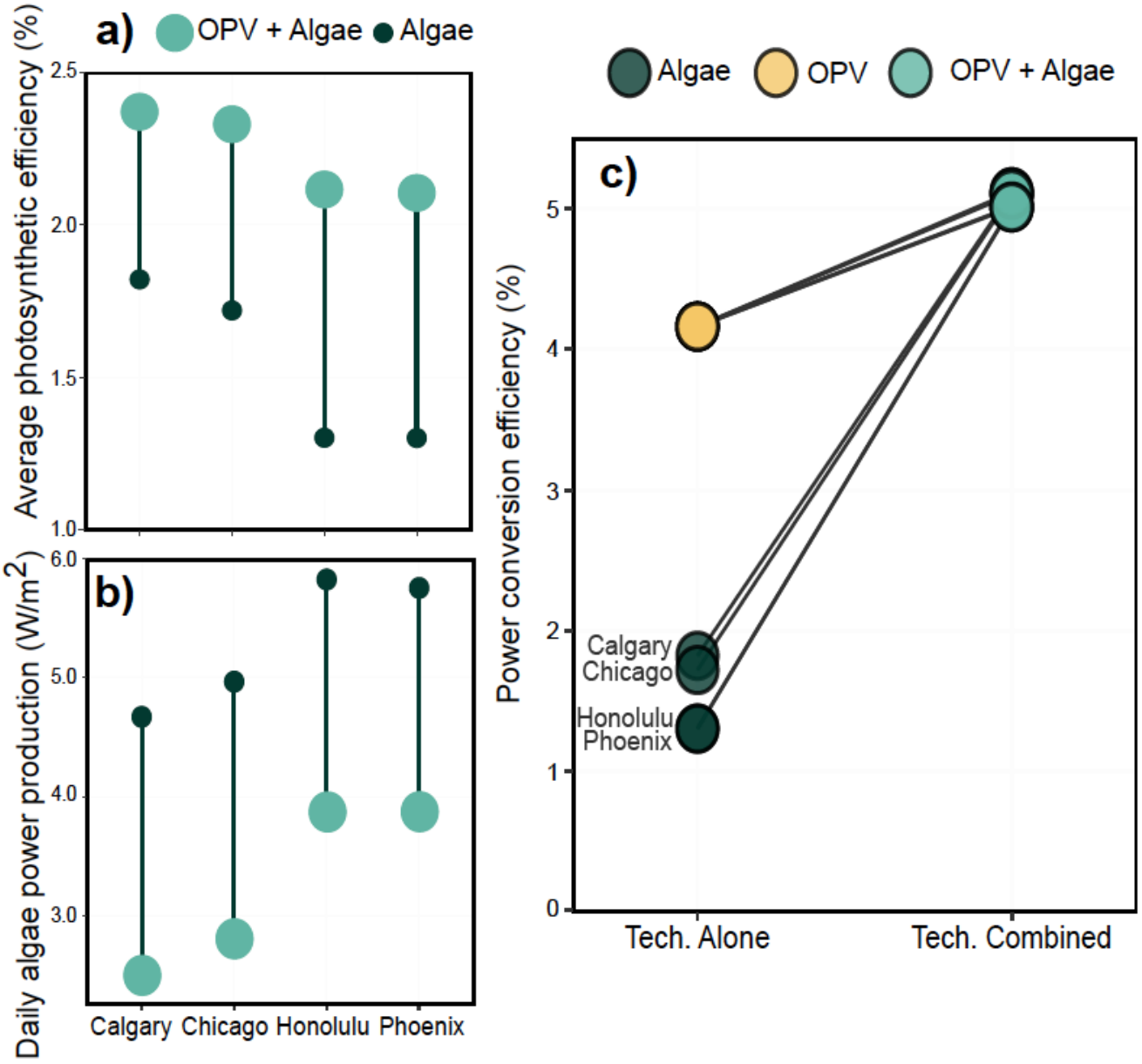

Figure 5

Solar conversion efficiencies and algal growth. a) Average annual photosynthetic efficiency of algae grown with OPV light filtration (light green), and without (dark green). b) Average annual power production of algae grown with OPV light filtration (light green), and without (dark green). c) Solar conversion efficiency of algal photosynthesis (dark green), OPV (yellow), and both technologies combined (light green). Values displayed are the average between 0.1 and 0.5 g/L cultures.

Supplementary Files

This is a list of supplementary files associated with this preprint. Click to download.

- SupplementaryInformation.pdf